

## Original Article

# The diagnostic value of 3.0T MRI in cesarean scar pregnancy

Shuning Guo<sup>1</sup>, Haitao Wang<sup>1</sup>, Xiuying Yu<sup>2</sup>, Yang Yu<sup>3</sup>, Chunguo Wang<sup>4</sup>

<sup>1</sup>Department of Radiology, Linyi Central Hospital, Linyi 276400, Shandong Province, China; <sup>2</sup>Department of Imaging, Linyi Hospital of Traditional Chinese Medicine, Linyi 276003, Shandong Province, China; <sup>3</sup>Department of Radiology, Beijing Changping District Hospital, Changping 102200, Beijing, China; <sup>4</sup>Department of Radiology, Women's and Children's Health Care Hospital of Linyi, Linyi 276016, Shandong Province, China

Received February 7, 2021; Accepted February 24, 2021; Epub June 15, 2021; Published June 30, 2021

**Abstract:** Objective: The purpose was to evaluate the diagnostic value of 3.0T MRI in cesarean scar pregnancy (CSP). Methods: 56 patients with suspected CSP treated in our hospital from August 2018 to July 2020 were recruited as the study cohort and diagnosed using ultrasound and 3.0T MRI. With the pathological examination results as the gold standard and the ultrasound examination results as a comparison, the diagnostic value of 3.0T MRI was evaluated according to the diagnostic accuracy, sensitivity, specificity, and positive and negative misdiagnosis rates, etc. Results: The pathological examination showed that 33 patients were positive for CSP but the other 23 were negative. The accuracy, sensitivity, and specificity of 3.0T MRI in the CSP diagnoses were significantly higher than the accuracy, sensitivity, and specificity of the ultrasound diagnoses ( $P < 0.05$ ), and the positive and negative misdiagnosis rates were significantly lower than the misdiagnosis rates of the ultrasound diagnosis ( $P < 0.05$ ). Moreover, the images from two patients showed that 3.0T MRI can provide clear images of the patients' lesion locations. Conclusion: Compared with ultrasound diagnoses, 3.0T MRI has significant advantages in diagnosing CSP and has a high clinical value.

**Keywords:** 3.0T MRI, cesarean scar pregnancy, ultrasound diagnosis, sensitivity, specificity

## Introduction

Cesarean scar pregnancy (CSP) refers to an ectopic pregnancy in which a patient's endometrium forms a scar due to factors such as a cesarean section or inflammation, with the blastocyst implantation at the scar in the subsequent pregnancy [1-3]. With a long latency and no obvious clinical features in the early stage, this disease can cause a uterine rupture and then lead to massive hemorrhaging, which takes a toll on patients [4-6]. Therefore, the early diagnosis and treatment of scar pregnancy has become a concern. At present, ultrasound diagnosis is the main method of detecting CSP. However, studies have shown that there is a certain misdiagnosis rate with single ultrasound diagnoses, which can easily cause a missed diagnosis or the misdiagnosis of patients, thus affecting the efficiency of the clinical diagnosis to a certain extent [7-10]. By comparing the effects of ultrasound and 3.0T

MRI in the diagnosis of CSP, this study aims to evaluate the clinical effectiveness of 3.0T MRI.

## Materials and methods

### General information

56 patients with suspected CSP treated in our hospital from August 2018 to July 2020 were recruited as the study cohort. They ranged in age from 25 to 43 years old and had no serious adverse diseases, and they were administered a course of *Leonurus* to help them adjust after their last cesarean section. Their baseline information is shown in **Table 1**.

### Inclusion and exclusion criteria

**Inclusion criteria:** (1) This study was approved by the hospital ethics committee (approval No. SWYX2018-307), and the patients and their families were given a full explanation of this experiment and of the potential risks in the

### 3.0T MRI in cesarean scar pregnancy

**Table 1.** General patient information (n=56)

General patient information	
Age (years old)	25-43
Average age (years old)	31.3±3.2
One cesarean section	37
Two cesarean sections	13
Three cesarean sections	6
Menstrual stop time (days)	55.3±7.5
Number of serious diseases (cases)	0

**Table 2.** Comparison of the 3.0T MRI and ultrasound results

Diagnostic method	3.0T MRI			Ultrasound		
	Pathological results		Total	Pathological results		Total
	Positive	Negative		Positive	Negative	
Positive	31	2	33	24	8	32
Negative	2	21	23	9	15	24
Total	33	23	56	33	23	56

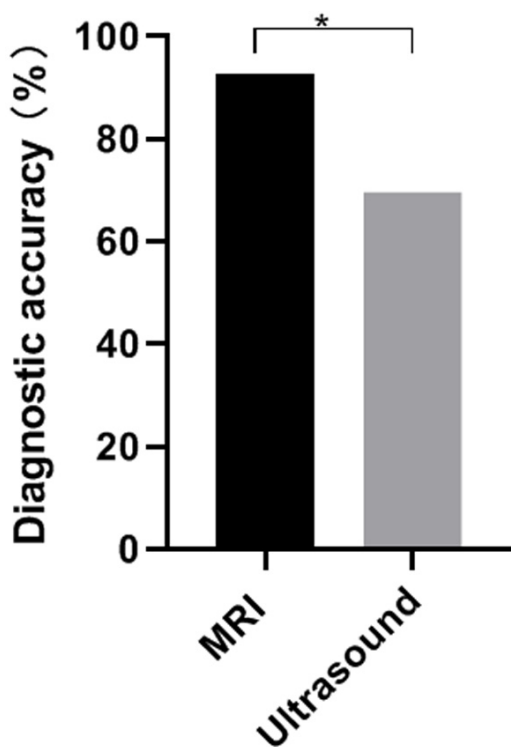


**Figure 1.** Comparison of the accuracy between 3.0T MRI and ultrasound. Note: The abscissa represents the diagnostic methods and the ordinate represents the CSP diagnostic accuracy. The accuracy rates of 3.0T MRI and ultrasound were 92.86% and 69.64% respectively ( $\chi^2=9.90$ ;  $P<0.01$ ).

process. (2) The patients signed the informed consent forms while they were alert and accompanied by their family members. (3) The

patients had no allergies to the drugs involved and no contraindications to the 3.0T MRI examination.

*Exclusion criteria:* (1) Patients with incomplete pathological data or ambiguous information. (2) Patients unwilling to cooperate during the treatment or the follow-up. (3) Patients with other diseases that seriously affected the experimental results.

#### Methods

**3.0T MRI diagnosis.** An Ingenia 3.0T superconducting magnetic resonance apparatus (PHILIPS company) was used. The patients took a supine position, received breathing training before the scanning to alleviate the tension, and were scanned in a quiet environment. The scanning range was from the pelvic pubis to the bottom of the uterus, including the entire pelvic region. The scan sequences were as follows:

(1) Horizontal axis parameters of T1WI-TSE sequence: TR 563 ms, TE 20 ms, 5 mm of slice thickness, 1 mm of spacing, FOV 250 × 250 mm<sup>2</sup> and Matix 344 × 307. (2) Horizontal axis parameters of T2WI-MVXD: TR 3000 ms, TE 100 ms, 5 mm of slice thickness, 1 mm of spacing, FOV 250 × 250 mm<sup>2</sup> and Matix 252 × 252. (3) Horizontal axis parameters of T2WI-SPIR: TR3203 ms, TE 100 ms, 5 mm of slice thickness, 1 mm of spacing, FOV 350 × 350 mm<sup>2</sup> and Matix 388 × 325. (4) Sagittal parameters of T2WI-MVXD: TR 3384 ms, TE 92 ms, 5 mm of slice thickness, 1 mm of spacing, FOV 250 × 250 mm<sup>2</sup> and Matix 312 × 312. (5) Coronal position parameters of the T2WI-TSE sequence: TR 4241 ms, TE 100 ms, 5 mm of slice thickness, 1 mm of spacing, FOV 250 × 250 mm<sup>2</sup> and Matix 356 × 341. (6) Horizontal axis parameters of DWIBS50/400/800: TR4642 ms, TE 70 ms, 5 mm of slice thickness, 1 mm of spacing, FOV 300 × 300 mm<sup>2</sup>, Matix 88 × 86, and three B values as 50 s/mm<sup>2</sup>, 400 s/mm<sup>2</sup> and 800 s/mm<sup>2</sup> respectively. A fat saturation sagittal thin-layer multiphase sequence of T1WI\_mDIXON was used for the enhancement scanning, with a total of 8 phases for scanning and the parameters set at TR 3.9 ms, TE1/TE2 1.31/2.3 ms, 2.5 mm of slice

(1) Horizontal axis parameters of T1WI-TSE sequence: TR 563 ms, TE 20 ms, 5 mm of slice thickness, 1 mm of spacing, FOV 250 × 250 mm<sup>2</sup> and Matix 344 × 307. (2) Horizontal axis parameters of T2WI-MVXD: TR 3000 ms, TE 100 ms, 5 mm of slice thickness, 1 mm of spacing, FOV 250 × 250 mm<sup>2</sup> and Matix 252 × 252. (3) Horizontal axis parameters of T2WI-SPIR: TR3203 ms, TE 100 ms, 5 mm of slice thickness, 1 mm of spacing, FOV 350 × 350 mm<sup>2</sup> and Matix 388 × 325. (4) Sagittal parameters of T2WI-MVXD: TR 3384 ms, TE 92 ms, 5 mm of slice thickness, 1 mm of spacing, FOV 250 × 250 mm<sup>2</sup> and Matix 312 × 312. (5) Coronal position parameters of the T2WI-TSE sequence: TR 4241 ms, TE 100 ms, 5 mm of slice thickness, 1 mm of spacing, FOV 250 × 250 mm<sup>2</sup> and Matix 356 × 341. (6) Horizontal axis parameters of DWIBS50/400/800: TR4642 ms, TE 70 ms, 5 mm of slice thickness, 1 mm of spacing, FOV 300 × 300 mm<sup>2</sup>, Matix 88 × 86, and three B values as 50 s/mm<sup>2</sup>, 400 s/mm<sup>2</sup> and 800 s/mm<sup>2</sup> respectively. A fat saturation sagittal thin-layer multiphase sequence of T1WI\_mDIXON was used for the enhancement scanning, with a total of 8 phases for scanning and the parameters set at TR 3.9 ms, TE1/TE2 1.31/2.3 ms, 2.5 mm of slice

### 3.0T MRI in cesarean scar pregnancy

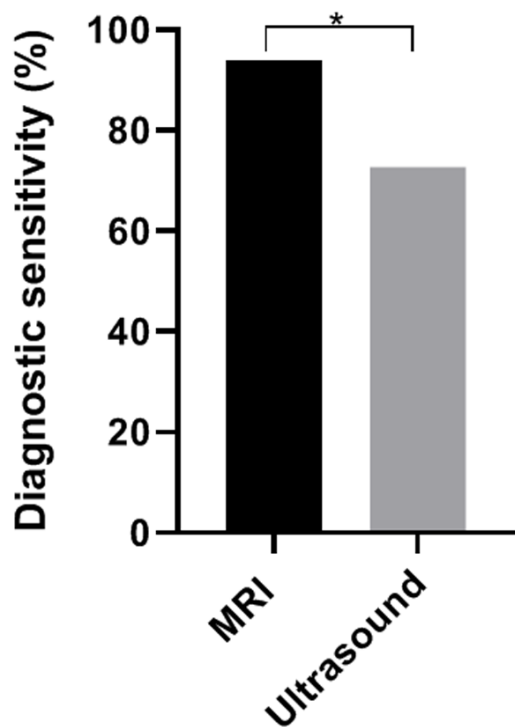


**Figure 2.** Comparison of the sensitivity between 3.0T MRI and ultrasound. Note: The abscissa represents the diagnostic methods and the ordinate represents the CSP diagnostic sensitivity. The sensitivity rates of the 3.0T MRI and the ultrasound were 93.94% and 72.73% respectively ( $\chi^2=4.65$ ,  $P<0.05$ ).

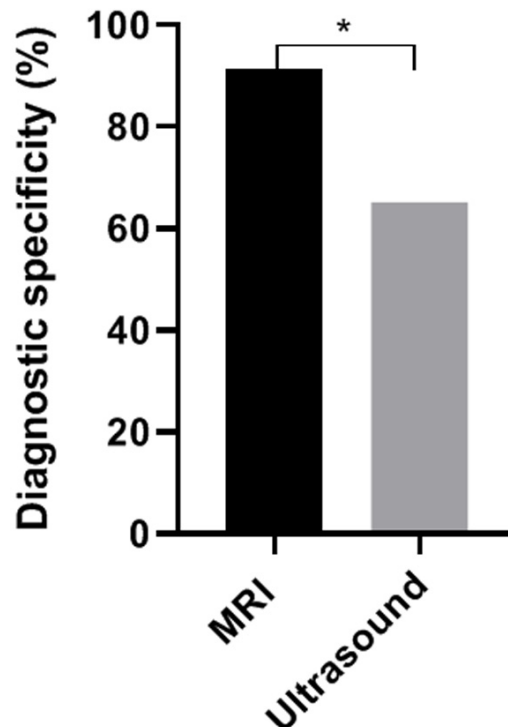


**Figure 3.** Comparison of the specificity between 3.0T MRI and ultrasound. Note: The abscissa represents the diagnostic methods and the ordinate represents the CSP diagnostic specificity. The specificity rates of the 3.0T MRI and the ultrasound were 91.30% and 65.22% respectively ( $\chi^2=4.60$ ,  $P<0.05$ ).

thickness, FOV  $300 \times 300 \text{ mm}^2$  and Matix 268  $\times 188$ . Then the transverse and coronal T1WI\_SPIR was scanned. The contrast agent was gadopentetate monomeglumine (Gd-DTPA), with a flow rate of 1.8 ml/s (0.1 mmol/kg body weight), which was injected into the patients with a high pressure syringe via the elbow vein.

**Ultrasound diagnosis.** After the patients drank an appropriate amount of water to ensure bladder filling, a GE73 ultrasonic diagnostic apparatus (GE Company, USA) was used for the diagnosis and detection. In the ultrasound detection, the frequency ranges of the trans-abdominal and vaginal probes were 3.0-5.0 Hz and 5-7 Hz respectively. After the probe penetrated into the vagina, the position, size and echo characteristics of the gestational sac and the scar tissue were observed.

#### Diagnostic methods

Independent diagnoses were performed by two professional radiologists who had 10-year experience. Whether the patients were posi-

tive for CSP was determined by the scar locations and the locations, sizes, and signal characteristics of the gestational sac.

#### Data processing

The data in this study were analyzed using SPSS 20.0 (IBM Corp. Released 2013. IBM SPSS Statistics for Windows, Version 22.0. Armonk, NY: IBM Corp) and the graphs were plotted with GraphPad Prism 8.0 (GraphPad Software, San Diego, CA, USA). The count data were tested using  $\chi^2$  tests, and the measurement data were tested using t tests. The statistical significance was set as a  $P$  value of 0.05 or lower.

#### Results

##### The 3.0T MRI and ultrasound diagnostic results

The results of the 3.0T MRI and ultrasound are shown in **Table 2**. The pathological exami-

### 3.0T MRI in cesarean scar pregnancy

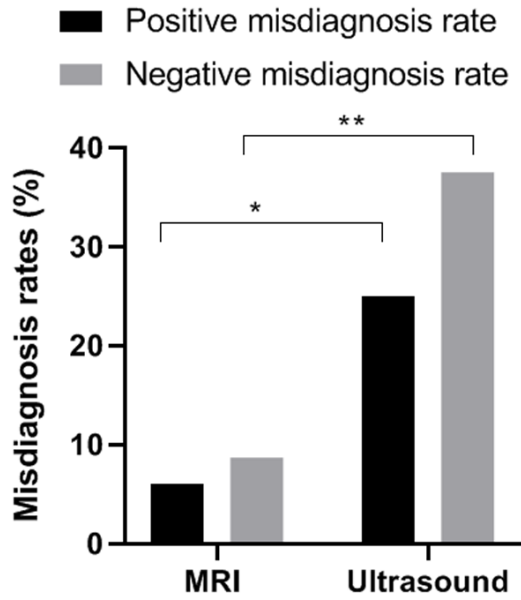


**Figure 4.** Comparison of the positive and negative misdiagnosis rates of 3.0T MRI and ultrasound. Note: The abscissa represents the diagnostic methods and the ordinate represents the positive and negative CSP misdiagnosis rates. The positive misdiagnosis rates of 3.0T MRI and ultrasound were 6.06% and 25.00% respectively ( $\chi^2=4.48$ ,  $P<0.05$ ). The negative misdiagnosis rates of 3.0T MRI and ultrasound were 8.70% and 37.50% respectively ( $\chi^2=5.44$ ,  $P<0.05$ ).

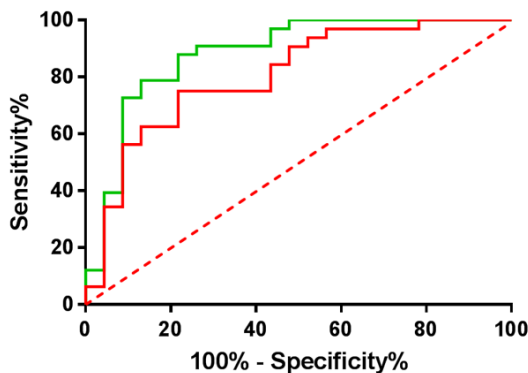


**Figure 5.** An ROC curve analysis of 3.0T MRI and ultrasound. The AUCs of 3.0T MRI and ultrasound were 0.883 and 0.804, respectively.

nation confirmed that 33 of the 56 patients were positive for human chorionic gonadotropin (HCG) and they were also confirmed to be positive for CSP, and 23 patients were confirmed to be negative for CSP. In the ultrasound examinations, 32 patients were identified as CSP patients, and 24 were identified as normal. In the 3.0T MRI examinations, 33

patients were identified as having CSP, and 23 were identified as normal. The 33 positive cases and 21 negative cases in the 3.0T MRI results were the same as in the pathological results, and the 24 positive cases and 15 negative cases were the same as in the pathological results. Both of the two diagnostic methods had some deviations from the pathological examination results.

#### *Comparison of the accuracy between MRI and ultrasound*

The accuracy of two diagnostic methods is shown in **Figure 1**. The accuracy rates of the 3.0T MRI and the ultrasound were 92.86% and 69.64% respectively, and the accuracy of the 3.0T MRI for CSP was significantly higher than the accuracy of the ultrasound diagnosis ( $P<0.01$ ).

#### *Comparison of sensitivity between 3.0T MRI and ultrasound*

The sensitivity rates of the two diagnostic methods are shown in **Figure 2**. The sensitivity rates of the 3.0T MRI and the ultrasound were 93.94% and 72.73% respectively, so the sensitivity of 3.0T MRI for CSP was significantly higher than the sensitivity of the ultrasound diagnosis ( $P<0.05$ ).

#### *Comparison of specificity between 3.0T MRI and ultrasound*

The specificity rates of the two diagnostic methods are shown in **Figure 3**. The specificity rates of the 3.0T MRI and the ultrasound were 94.29% and 65.22% respectively, and the specificity of the 3.0T MRI for CSP was significantly higher than the specificity of the ultrasound diagnosis ( $P<0.05$ ).

#### *Comparison of the misdiagnosis rates between 3.0T MRI and ultrasound*

The positive and negative misdiagnosis rates of the two diagnoses are shown in **Figure 4**. The positive misdiagnosis rates of the 3.0T MRI and the ultrasound were 6.06% and 25.00% respectively, and the negative misdiagnosis rates were 8.70% and 37.50% respectively. Moreover, the misdiagnosis rates of the 3.0T MRI for CSP were significantly lower than the misdiagnosis rates of the ultrasonic diagnosis ( $P<0.05$ ).

### 3.0T MRI in cesarean scar pregnancy

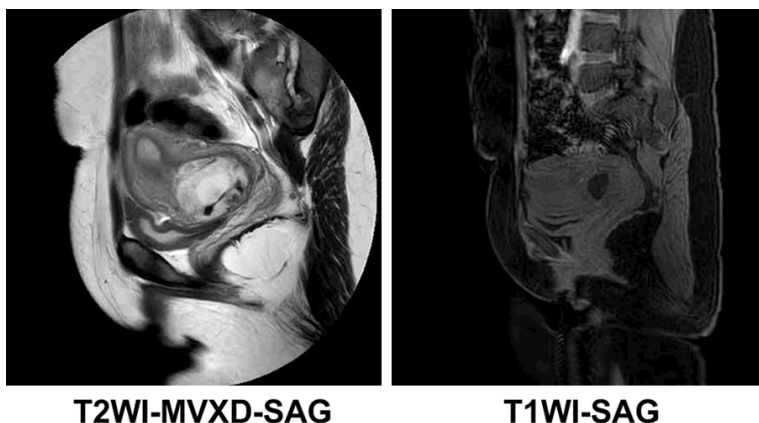


**Figure 6.** 3.0T MRI images of a patient with CSP.

#### *An ROC curve analysis of 3.0T MRI and ultrasound*

The ROCs of the two diagnoses are shown in **Figure 5**. The AUCs of the 3.0T MRI and the ultrasound were 0.883 and 0.804, respectively.

#### *Typical cases*

**Case 1:** A 33 year old female patient with type III CSP examined on September 12, 2019 (**Figure 6**). Imaging manifestations: The local mixed signal areas (about 4.20 cm × 4.75 cm × 4.12 cm) were seen in the scars of the anterior position of the uterus, the lower part of the uterine cavity, and the anterior inferior wall, with equally high and low mixed signals of T1WI and FST2WI, high and low mixed signals of DWI, local protrusions, and thin and discontinuous muscular layers. A dynamic enhancement showed a significant enhancement of the posterior and inferior lesion walls, implantation in the scars, fat spaces between the lower uterine segment and the bladder, and no significant abnormal signal shadow in the bilateral adnexal areas.

**Case 2:** A 36 year old female with type III CSP examined on October 5, 2018 (**Figure 7**). Imaging manifestations: The local mixed signal areas were seen in the scars of the posterior position of the uterus and the anterior inferior wall, with equally high T1WI signals, equally high and low mixed FST2WI signals, high and low mixed DWI signals, local protrusions, and a discontinuous muscular layer. The dynamic enhancement showed a significant enhance-

ment of the anterior walls of the lesions, no significant fat space between the lower uterine segment and the bladder, no significant abnormal morphological signals of the cervix, and no significant abnormal signal shadows in the bilateral adnexal areas.

#### **Discussion**

At present, the main treatments for CSP mainly focus on drug intervention or the surgical termination of pregnancy at the early stage of

embryo implantation, thus reducing the risk of uterine rupture and massive hemorrhaging caused by the invasion of the placenta into the uterus [11-13]. However, early CSP often has no obvious clinical symptoms [14, 15]. In order to improve the diagnostic efficiency of CSP, ultrasound diagnosis is usually performed on patients in the early stages of pregnancy and with a history of cesarean sections or surgery, which can prevent and control CSP to a certain extent [16-18]. Nevertheless, studies have shown that there are often some missed diagnoses or misdiagnoses in the detection of CSP by ultrasound diagnosis, which to some extent affects the efficiency of the clinical diagnosis [19].

In recent years, MRI has been widely used in some clinical diagnoses, especially in the diagnosis of carotid plaques and ectopic pregnancies [20]. As a safe gestational imaging method that does not require contrast agents and is lightly affected by the patient's physical constitution and other conditions, 3.0T MRI is considered to have a high clinical effectiveness in diagnosis [21]. The results of this study showed that the accuracy of 3.0T MRI in the diagnosis of CSP is significantly higher than the accuracy of ultrasound. Hoffmann et al. [22] used 3.0T MRI and ultrasound to diagnose 25 CSP patients, and their comparison of the two diagnostic methods showed that there was a significant difference between the diagnostic results of 3.0T MRI and ultrasound. Also, the imaging effect of 3.0T MRI was better, which could clearly image the uterine scar in 44% of the patients and had a high accuracy in measuring the wall thickness of the lower uterus.

### 3.0T MRI in cesarean scar pregnancy

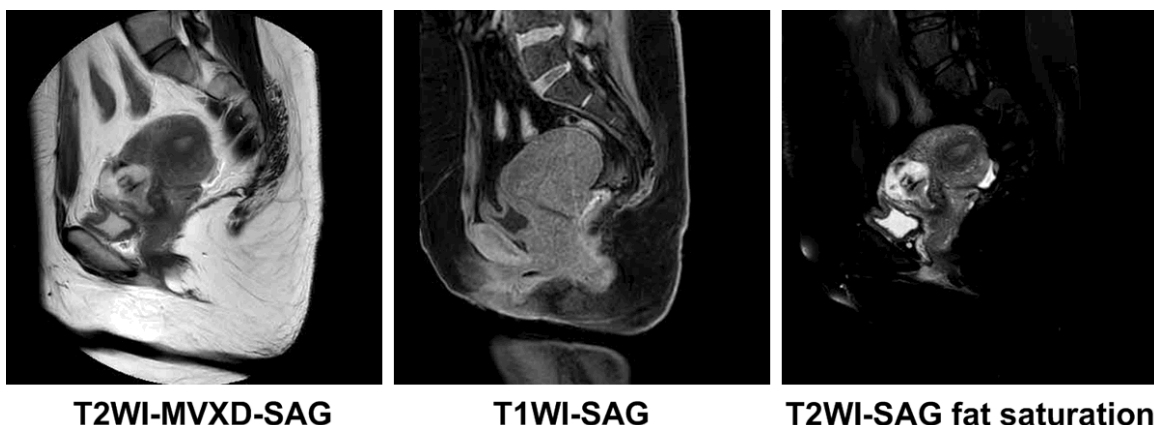


Figure 7. 3.0T MRI images of a patient with CSP.

Therefore, we believe that 3.0T MRI has a high reliability in the diagnosis of CSP. Additionally, 3.0T MRI has many advantages for CSP diagnosis, as it can image the patients' tissues from multiple directions and sequences. Compared with ultrasound, 3.0T MRI can capture the details of the lesions efficiently through high-definition imaging [23, 24]. This study found that, compared with ultrasound diagnosis, 3.0T MRI has significant advantages in terms of specificity, sensitivity, and in the prevention of misdiagnoses in detecting CSP. Hoffmann et al. [25] used 3.0T MRI and ultrasound to diagnose 164 patients and found that the ultrasound diagnostic method cannot accurately determine the thickness and morphology of the lower uterus in some special cases, but the high-definition imaging of 3.0T MRI can make up for this shortcoming to some extent.

In conclusion, compared with ultrasound, 3.0T MRI has a better diagnostic effect in the diagnosis of CSP, and it has a higher clinical value. However, due to the relatively small size of our study cohort and other factors such as geographic restrictions, the results of this study are not representative to some extent. However, the methods and operations of the diagnoses in this study are in line with medical standards, so we believe that the limitation is negligible.

#### Disclosure of conflict of interest

None.

**Address correspondence to:** Chunguo Wang, Department of Radiology, Women's and Children's

Health Care Hospital of Linyi, No. 1 Qinghe South Road, Linyi 276016, Shandong Province, China. Tel: +86-13696398138; E-mail: wangchunguo1234@126.com

#### References

- [1] Singh D and Kaur L. When a cesarean section scar is more than an innocent bystander in a subsequent pregnancy: ultrasound to the rescue. *J Clin Ultrasound* 2017; 45: 319-327.
- [2] Sokołowska M, Rajewska A, Mikołajek-Bedner W, Lebdowicz J, Nurek K, Kwiatkowski S and TorbÉ A. Cesarean scar pregnancy - case reports and literature review. *Pol Merkur Lekarski* 2020; 48: 179-183.
- [3] Di Spiezio Sardo A, Saccone G, McCurdy R, Bujold E, Bifulco G and Berghella V. Risk of Cesarean scar defect following single- vs double-layer uterine closure: systematic review and meta-analysis of randomized controlled trials. *Ultrasound Obstet Gynecol* 2017; 5: 578-583.
- [4] Kiyokawa S, Chiyoda T, Ueno K, Saotome K, Kim SH and Nakada S. Development of pseudoaneurysm in cesarean section scar pregnancy: a case report and literature review. *J Med Ultrason* 2018; 45: 357-362.
- [5] Maheux-Lacroix S, Li F, Bujold E, Nesbitt-Hawes E, Deans R and Abbott J. Cesarean scar pregnancies: a systematic review of treatment options. *J Minim Invasive Gynecol* 2017; 24: 915-925.
- [6] Ravi Selvaraj L, Rose N and Ramachandran M. Pitfalls in ultrasound diagnosis of cesarean scar pregnancy. *J Obstet Gynaecol India* 2018; 68: 164-172.
- [7] Liu D, Gu X, Liu F, Shi F, Yang M and Wu Q. Application of contrast-enhanced ultrasound for scar pregnancy cases misdiagnosed as other diseases. *Clin Chim Acta* 2019; 496: 134-139.
- [8] Tatli F, Gozeneli O, Uyanikoglu H, Uzunkoy A, Yalcin HC, Ozgonul A, Bardakci O, Incebiyik A

### 3.0T MRI in cesarean scar pregnancy

- and Guldur ME. The clinical characteristics and surgical approach of scar endometriosis: a case series of 14 women. *Bosn J Basic Med Sci* 2018; 18: 275-278.
- [9] Tadesse WG and Von Bunau G. A combination of surgery and methotrexate for successful treatment of a cesarean scar pregnancy. *Ir Med J* 2018; 111: 774.
- [10] Zhou LY, Zhu XD, Jiang J and Jiang TA. Uterine mass after caesarean section: a report of two cases. *BMC Pregnancy Childbirth* 2020; 20: 508.
- [11] Li YY, Yin ZY, Li S, Xu H, Zhang XP, Cheng H, Du L, Zhou XY and Zhang B. Comparison of transvaginal surgery and methotrexate/mifepristone-combined transcervical resection in the treatment of cesarean scar pregnancy. *Eur Rev Med Pharmacol Sci* 2017; 21: 2957-2963.
- [12] Pan Y and Liu MB. The value of hysteroscopic management of cesarean scar pregnancy: a report of 44 cases. *Taiwan J Obstet Gynecol* 2017; 56: 139-142.
- [13] Pristavu A, Vinturache A, Mihalceanu E, Pintilie R, Onofriescu M and Socolov D. Combination of medical and surgical management in successful treatment of cesarean scar pregnancy: a case report series. *BMC Pregnancy Childbirth* 2020; 20: 617.
- [14] Ndubizu C, McLaren RA Jr, McCalla S and Irani M. Recurrent cesarean scar ectopic pregnancy treated with systemic methotrexate. *Case Rep Obstet Gynecol* 2017; 2017: 9536869.
- [15] Calí G, Timor-Tritsch IE, Forlani F, Palacios-Jarquemade J, Monteagudo A, Kaelin Agten A, Flacco ME, Khalil A, Buca D, Manzoli L, Liberati M and D'Antonio F. Value of first-trimester ultrasound in prediction of third-trimester sonographic stage of placenta accreta spectrum disorder and surgical outcome. *Ultrasound Obstet Gynecol* 2020; 55: 450-459.
- [16] Xiao J, Shi Z, Zhou J, Ye J, Zhu J, Zhou X, Wang F and Zhang S. Cesarean scar pregnancy: comparing the efficacy and tolerability of treatment with high-intensity focused ultrasound and uterine artery embolization. *Ultrasound Med Biol* 2017; 43: 640-647.
- [17] Hsu CC and Huang KG. Evolving cesarean scar pregnancy into morbidity adherent placenta-evidence from serial ultrasound examination. *J Med Ultrasound* 2017; 25: 47-51.
- [18] Kaelin Agten A, Cali G, Monteagudo A, Oviedo J, Ramos J and Timor-Tritsch I. The clinical outcome of cesarean scar pregnancies implanted "on the scar" versus "in the niche". *Am J Obstet Gynecol* 2017; 216: 510.e1-510.e6.
- [19] Li H, Liu X, Xie L, Ye Z and Gan L. Diagnostic accuracy and cut-off of contrast-enhanced ultrasound in caesarean scar pregnancy. *Eur J Obstet Gynecol Reprod Biol* 2020; 246: 117-122.
- [20] Park BH, Marches S, Eichelberger BM, Winter MD, Pozzi A and Banks SA. Quantifying dog meniscal volume at 1.5T and 3.0T MRI. *Res Vet Sci* 2020; 128: 236-241.
- [21] Braileanu M, Wicks JM and Saindane AM. Appearance of an unusual ring enhancing brain capillary telangiectasia on 3.0T MRI with dynamic susceptibility contrast perfusion. *Radiol Case Rep* 2020; 15: 1331-1334.
- [22] Hoffmann J, Exner M, Bremicker K, Grothoff M, Stumpp P, Schrey-Petersen S and Stepan H. Cesarean section scar in 3T magnetic resonance imaging and ultrasound: image characteristics and comparison of the methods. *Arch Gynecol Obstet* 2019; 299: 439-449.
- [23] Zhang W and Chen J. Diffusion tensor imaging (DTI) of the cesarean-scarred uterus in vivo at 3T: comparison study of DTI parameters between nonpregnant and pregnant cases. *J Magn Reson Imaging* 2020; 51: 124-130.
- [24] Takeda A, Koike W, Imoto S and Nakamura H. Conservative management of uterine artery pseudoaneurysm after laparoscopic-assisted myomectomy and subsequent pregnancy outcome: case series and review of the literature. *Eur J Obstet Gynecol Reprod Biol* 2014; 182: 146-53.
- [25] Hoffmann J, Exner M, Bremicker K, Grothoff M, Stumpp P and Stepan H. Comparison of the lower uterine segment in pregnant women with and without previous cesarean section in 3T MRI. *BMC Pregnancy Childbirth* 2019; 19: 160.